# IL-25 axis is involved in the pathogenesis of human primary and experimental Sjögren's syndrome

| | |
|---|---|
| Journal: | *Arthritis & Rheumatology* |
| Manuscript ID | ar-17-1350.R1 |
| Wiley - Manuscript type: | Full Length |
| Date Submitted by the Author: | 08-Jan-2018 |
| Complete List of Authors: | Guggino, Giuliana; University of Palermo, Dipartimento di Biopatologia e Biotecnologie Mediche e Forensi<br>Lin, Xiang; The University of Hong Kong, Pathology<br>Rizzo, Aroldo; Azienda Ospedaliera Ospedali Riuniti Villa Sofia e Cervello, Anatomia Patologica<br>Xiao, Fan; Pathology<br>Saieva, Laura; University of Palermo, Dipartimento di Biopatologia e Biotecnologie Mediche e Forensi<br>Raimondo, Stefania; University of Palermo, Dipartimento di Biopatologia e Biotecnologie Mediche e Forensi<br>Di Liberto, Diana; University of Palermo<br>Candore, Giuseppina; Universita degli Studi di Palermo<br>Ruscitti, Piero; Università di L'Aquila, Italy, Dipartimento di Scienze Cliniche Applicate e Biotecnologiche, Sezione di Reumatologia<br>Cipriani, Paola; University of L'Aquilaa, Department of Internal Medicine and Public Health, Section of Rheumatology<br>Giacomelli, Roberto; University of L'Aquilaa, Department of Internal Medicine and Public Health, Section of Rheumatology<br>Dieli, Francesco; University of Palermo, Dipartimento di Biopatologia e Biotecnologie Mediche e Forensi<br>Alessandro, Riccardo; University of Palermo, Dipartimento di Biopatologia e Biotecnologie Mediche e Forensi<br>Triolo, Giovnni; University of Palermo, Dipartimento Biomedico di Medicina Interna e Specialistiche<br>Lu, Liwei; The University of Hong Kong, Pathology and Center of Infection and Immunology<br>Ciccia, Francesco; Rheumatology Unit, Dipartimento Biomedico di Medicina Interna e Specialistiche; |
| Keywords: | Sjögren's Syndrome, Cytokines |
| <B>Disease Category</b>: Please select the category from the list below that best describes the content of your manuscript.: | Sjögren s Syndrome |
| | |

# IL-25 axis is involved in the pathogenesis of human primary and experimental Sjögren's syndrome

First Author's name: Guggino Running Title: IL-25 in pSS

*Giuliana Guggino[1] MD,PhD, *Xiang Lin PhD[2] , Aroldo Rizzo[3] MD, Fan Xiao BSC[2], Laura Saieva[4] PhD, Stefania Raimondo[4] PhD, Diana Di Liberto[4] PhD, Giuseppina Candore[4] PhD, Piero Ruscitti[5] MD, Paola Cipriani[5] MD, PhD, Roberto Giacomelli[5] MD,PhD, Francesco Dieli[4] MD,PhD, Riccardo Alessandro[4] PhD, Giovanni Triolo[1] MD, #Liwei Lu[3] PhD, #Francesco Ciccia[1] MD,PhD,

*GG and XL contributed equally to this work

#LL and FC shared co-senior autorship

[1]Dipartimento Biomedico di Medicina Interna e Specialistica, Sezione di Reumatologia, University of Palermo, Palermo, Italy

[2] Department of Pathology, University of Hong-Kong,

[3] Anatomia Patologica, Ospedali riuniti Villa Sofia-Cervello, Palermo, Italy

[4]Dipartimento di Biopatologia e Biotecnologie Mediche, Università di Palermo, Palermo, Italy

[5]Dipartimento di Scienze Cliniche Applicate e Biotecnologiche, Sezione di Reumatologia, Università di L'Aquila, Italy

Correspondence:

Dr Francesco Ciccia, Department of Internal Medicine, Division of Rheumatology, Piazza delle Cliniche 2, 90127 Palermo, Italy; francesco.ciccia@unipa.it; Tel: (39) 0916552189

Prof. Liwei Lu, Department of Pathology, University of Hong-Kong, Queen Mary Hospital, Pokfulam Road, Hong Kong liweilu@hku.hk; Tel: (852) 2255-3967

**Disclosures:** The authors declare no competing interests

**Abstract**

**Objective:** To investigate the role of IL-25/IL-17RB axis in experimental Sjögren's syndrome (ESS) and in patients with primary Sjögren Syndrome (pSS) and pSS-associated lymphoma.

**Methods**: Expression of IL-25, IL-17RB, IL-17B and TRAF6 was analyzed on minor salivary glands (MSG) from pSS patients and on parotid glands from pSS-associated B cell non-Hodgkin lymphomas (NHL). IL-17RB expression and the frequencies of natural type 2 innate lymphoid cells (nILC2), inflammatory ILC2 (iILC2) and M2-polarized macrophages were assessed by flow cytometry in salivary gland mononuclear cells (SGMC) and peripheral blood mononuclear cells (PBMC). Tissue distribution of ILC2 cells was studied by confocal microscopy. The role of recombinant IL-25 and of Rituximab in modulating IL-25 expression was investigated in *in vitro* studies. IL-25/IL-17RB and TRAF6 expression and the role of IL-25 inhibition were also studied in the ESS murine model.

**Results**: activation of IL-25/IL-17RB/TRAF6 axis correlated with the focus score, was observed in pSS patients and in pSS-associated NHL. A significant increase in the frequency of iILC2 was observed in both SGMC and PBMC. IL-25 stimulation of isolated SGMC and PBMC from patients and controls resulted in both iILC2 expansion and increased autoantibodies production. Rituximab modulated iILC2 and IL-25 expression in pSS. Salivary gland protein-immunised mice developed overt SS symptoms with increased IL-25 expression and increased frequency of $CD4^+IL\text{-}17RB^+TRAF6^+$ cells. IL-25 neutralization attenuated disease progression and tissue pathology in ESS mice.

**Conclusions**: IL-25 may promote the inflammatory state in pSS and may be a potential target for novel disease-modyfing therapeutic strategies in pSS patients.

**Key words:** pSS, Experimental Sjogren Syndrome, IL-25, IL-17RB, ILC2

## Introduction

Primary Sjögren's syndrome (pSS) is a chronic systemic autoimmune disease characterized by an increased risk of developing lymphomas (1). pSS is thought to be essentially driven by a complex interplay between epithelial barrier and adaptive and innate immunity (2). In particular, type 2 adaptive immune responses have been shown in pSS, mainly dominated by the selective concentration of T helper 2 (Th2) cells in the context of germinal centers (GCs) and the increased salivary glands (SG) expression of IL-33 (3).

Recently, IL-25, a member of the IL-17 cytokine family, also known as IL-17E, has been implicated in the regulation of innate and adaptive immune responses, essentially by inducing a type 2 immunity (4); as IL-17B, IL-25 signals through the IL-17RB receptor expressed on epithelial and immune cells modulating several activities (5). Specifically, IL-25 regulates the development of the autoimmune inflammation mediated by IL-17-producing T cells (6). Furthermore, IL-25/IL-17RB activation promotes Th2 responses by increasing the frequency of M2-polarized macrophages (7) and the differentiation of both natural and inflammatory innate lymphoid cells of type 2 (ILC2) (8-9).

Despite of these pivotal functions in modulating immune responses, the role of IL-25/IL-17RB axis and of innate lymphoid cells of type 2 (ILC2) in the pathogenesis of experimental Sjögren's syndrome (ESS) and pSS, as well as in pSS-associated lymphoma has not been yet investigated.

In this study, we demonstrate that the IL-25/IL-17RB axis is activated in ESS, pSS and in pSS-associated lymphoma and this is associated, in humans, with the increased frequency of IL-25–responsive inflammatory ILC2 cells (iILC2) and M2 macrophages, together with an increased production of pSS-related autoantibodies. Our study suggests

that IL-25 may promote, by interacting locally and sistemically with IL-17RB$^+$ cells, innate and adaptive immune responses, thus modulating the inflammatory state in pSS.

**Methods**

*Experimental procedures in ESS*

The ESS mouse model was induced in 8-week-old female C57BL/6 mice by immunization with SG proteins as we previously described (10). In brief, proteins extracted from the bilateral SG of normal mice were emulsified in an equal volume of Freund's complete adjuvant (Sigma-Aldrich) to a concentration of 2 mg/ml. For SS induction, each mouse received subcutaneous multi-injections on the back of 0.1 ml of the emulsion on days 0 and 7, respectively. On day 14, the booster injection was carried out with a dose of 1 mg/ml SG proteins emulsified in Freund's incomplete adjuvant (Sigma-Aldrich). All experiments for animal studies were approved by the Committee on the Use of Live Animals in Teaching and Research of the University of Hong Kong.

Serum samples from ESS mice at various disease time points were collected and measured by IL-25 (eBioscience), IL-5 (Biolegend) and IL-13 (R&D Systems) ELISA kit following the manufactural instruction. Since increased IL-25 levels were only detectable at chronic stage, around 30wk post immunization, ESS mice were administrated with 200 μg of anti-IL-25 monoclonal antibody (35B, Biologend) or PBS vehicle via intraperitoneal injection before they entered chronic stages, at 20wk post immunization. Mice were treated twice every week for 4 wk. The saliva flow rate of ESS mice was assessed before and after anti-IL-25 treatment. SG tissues removed from immunised mice were frozen into OCT compound (Sakura) and sections were cut at 5 μm thickness. For immunofluoresce microscopy, frozen sections were stained with monoclonal antibodies against mouse CD4 (clone RM4-5, Biolegend) and IL-25 (clone 207702, R&D), while nuclei were counterstained with Hoechst 33258 (CalBioChem). Rat IgG antibody was used for control staining. For the flow cytometry experiments in ESS mice surface markers were identified

with following anti-mouse monoclonal antibodies: anti-CD4, anti-IL-17RB (clone 752101, R&D), anti-CD45 (30-F11, Biolegend), anti-F4/80 (BM8), anti-IL-7Rα (A7P34, Biolegend), anti-CD206 (C068C2, Biolegend) and anti-lineage markers (CD2, CD3, CD4, CD8, CD19, B220, Gr-1, CD11b, CD11c, FcεRI and TER119, Biolegend). Detection of intracellular IL-25 and TRAF6 (clone EP591Y, Abcam) was prepared by using a fixation/permeablization buffer set (BD Biosciences). Stained cells were analyzed with a LSRFortessa flow cytometer (BD Biosciences) while Zombie Aqua™ Live/Dead Cell Discrimination kit (Biolegend) was used to exclude the dead cells. Data were analyzed by FlowJo software (Treest).

*Patients*

Peripheral blood samples and minor labial salivary glands (MSG) biopsies were obtained from 50 patients (46 female, mean age 58 ± 12 years, mean disease duration 34 ± 12 months) displaying xerostomia and xerophtalmia and meeting the American–European Consensus Group (AECG) criteria (11) for pSS. All the patients enrolled were HCV negative. Thirthy patients with subjective complains of dry mouth or dry eyes who did not fulfill the AECG criteria and show various degree of mononuclear cell infiltration in the absence of focal organisation were classified as having non-specific chronic sialoadenitis (nSS) and were considered as control group. Paraffin-embedded samples obtained from patients with a previous diagnosis of pSS-associated MALT lymphoma (n=5) were obtained from the biopsy bank of the Pathology Unit of the Ospedale Cervello (Palermo, Italy). Diagnosis of lymphoma was made by the demonstration of sheets or halos of monocytoid B cells and by the demonstration of immunoglobulin(Ig)H and/or IgL chain restriction. Baseline characteristics of patients and controls are shown in Supplemental Table1. All the patients and controls gave their informed consent and the study was approved by the ethical committee of the University of Palermo. Multiple labial MSG biopsies were obtained from all the pSS patients and controls and placed into formalin

fixative and RNAlater for immunohistochemistry and reverse transcription–polymerase chain reaction (RT–PCR) analyses, respectively. Twenty paired biopsies, from patients and controls, were also placed in RPMI for isolation of SGMC and used for flow cytometry analysis.

*Histology and immunohistochemistry*

Paraffin-embedded sections of 5-μm thickness were stained with haematoxylin and eosin (H&E) for the histological evaluation of the presence of lymphocytic infiltrates performed according to Greenspan and coworkers (12). A focus was defined as an aggregate of ≥50 lymphocytes. The focus score was reported as the number of foci per 4 $mm^2$ of tissue, up to a maximum of 12 foci. All patients with pSS presented a biopsy focus score ≥1, whereas the control group had a focus score <1. The presence of GC-like lymphoid structures was determined by the presence of T and B lymphocytes and $CD21^+$ follicular dendritic cells networks on sequentially stained sections. Immunohistochemistry was performed on 5-μm-thick paraffin-embedded sections from SG as described previously (13). The primary antibodies mouse anti-human IL-25, rabbit anti-human IL-17RB, rabbit anti-human IL-17B (Novus Biologicals, Littleton, CA) and rabbit anti-human TRAF6 (Abcam, Cambridge, UK) were added and incubated for 1 h at room temperature. Isotype-matched irrelevant antibodies were used as a negative control (AbCam, Cambridge, UK). The number of positive cells was determined by counting the reactive cells on microphotographs obtained from three randomly selected high-power microscopic fields (original magnification ×400).

*Confocal microscopy analysis*

Triple stainings were performed on paraffin-embedded sections of MSG for CD3/Thy-1/IL-17RB (for ILC2) and CD68/CD163/c-maf (for M2 macrophages). The sections were treated with FITC-, Rhodamine Red or Cy-5-conjugated antimouse or antirabbit antibodies (Invitrogen), plus RNasi (200 ng/mL) and counterstained using 4′,6-diamidino-2-

phenylindole (DAPI) (Life Technologies). Confocal analysis was used to acquire fluorescence staining.

*RNA extraction from salivary gland biopsies and quantitative TaqMan RT–PCR*

Soon after removal, SG biopsies were also stored in RNAlater® solution (Applied Biosystems, Foster City, CA, USA). RT–PCR was performed as described previously.[13] Master mix and Taqman® gene expression assays for glyceraldehyde 3-phosphate dehydrogenase (GAPDH control) and target genes IL-25 (Hs03044841_m1), IL-17RB (Hs00218889_m1), IL-17B (Hs00975262_m1), IL-33 (Hs00369211_m1), Arg-1 (Hs00968979_m1) and GADPH (Hs02758991_g1) were obtained from Applied Biosystems (Foster City, CA, USA). Data were quantified using sds 2.1 software and normalized using GAPDH as endogenous control. Relative changes in gene expression between nSS and pSS samples were determined using the ΔΔCt method. Levels of the target transcript were normalized to a GAPDH endogenous control, constantly expressed in both groups (ΔCt). For ΔΔCt values, additional subtractions were performed between pSS (n = 50) and nSS (n = 20) ΔCt values. Final values were expressed as fold of induction.

*Isolation and culture of minor salivary gland mononuclear cells and flow cytometry*

Minor salivary gland mononuclear cells (SGMC) were obtained as described previously from 20 pSS and 20 nSS patients (13). Cell viability (trypan blue dye exclusion) was always > 95%. Cells were cultured with recombinant IL-25 (0.25 ug/ml) (R&D system, MN, US) for 24 h at 37°C in the presence of 5% $CO_2$. *In vitro* cultured cells were stained with the following antibodies: anti-human CD45, anti-human Lineage Cocktail (anti-human CD3, anti-human CD56, anti-human CD14, anti-human CD19, anti-human TCR-$\gamma\delta$, anti-human iNKT) anti-human IL-17RB, anti-human KLRG1 and anti-human Thy1, anti human GATA3, anti-human CRTH2, anti-human CD14 and anti-human CD68 (BD, Biolegend and R&D). Detection of intracellular IL-25 (R&D) and TRAF6 (Abcam) was performed using a

fixation/permeablization buffer set (BD Biosciences). Flow cytometry analysis was performed using a fluorescence activated cell sorter (FACS)Canto (BD Biosciences, San Jose, CA, USA). At least 50 000 cells (events), gated on the lymphocyte region, were acquired for each sample and data are presented as a percentage of total alive cells in the CD45 channel.

*Evaluation of anti-RoSSA and LaSSB autoantibodies following IL-25 stimulation*

The role of IL-25 in modulating the production of anti-RoSSA and LaSSB autoantibodies was performed as previously described (14). PBMC were obtained from the peripheral blood of anti-RoSSA$^{+}$ pSS patients after centrifugation on Ficoll-Hypaque (Pharmacia). The medium used throughout was RPMI 1640 (Invitrogen Life Technologies) supplemented with 10% heat-inactivated pooled human AB+ serum, 2 mM l-glutamine, 20 mM HEPES, 100 U/ml penicillin, 100 µg/ml streptomycin, $5 \times 10^{-5}$ M 2-ME. PBMC were cultured with or without recombinant-IL-25 (rIL-25: 0.25 ug/ml) in U-bottom 96-well plates and incubated at 37°C, 5% $CO_2$ for 72 hours. After incubation, supernatants were collected to test anti-RoSSA/LaSSB production by Immunoblot (Euroimmune).

*Statistical analysis*

Parametric and non-parametric statistical analysis was performed calculating the mean ± standard error of the mean (s.e.m.) and median, respectively. For comparison of parametric and non-parametric data, the *t*-test and Mann–Whitney rank-sum test were used where appropriate. Spearman's correlation analysis was utilized to quantify the expression associations between the genes of interest. *p*-values less than 0.05 were considered to be significant. For the experiments in ESS mice results are expressed as mean ± SD. Data were analyzed using Mann Whitney U test or One-way ANOVA to determine the difference between groups using SPSS16.0 (*$p < 0.05$ and **$p < 0.01$).

## Results

*IL-25 axis is activated in ESS*

To investigate the pathogenic role of IL-25 during ESS development, we first measured serum levels of IL-25 in ESS mice at various time points upon disease induction. Interestingly, serum levels of IL-25 were significantly increased at 30wk post-immunization (Fig. 1A),and were found further elevated along disease progression. To detect the IL-25 production in SG, harvested SG were digested for single-cell suspension, followed by the stimulation of PMA (50 ng/mL), inomycin (1 μg/mL) and monensin for 4 hours before flow cytometric analysis. A significant increase of IL-25-producing $CD45^-$ tissue cells was observed in ESS mice with lymphocytic infiltration in the SG when compared with those ESS mice without glandular infiltration and normal controls (Fig.1B). We further examined the IL-25-expressing cells *in situ* by confocal microscopy. IL-25 expression was detected in the tissue cells in the submandibular gland, mostly acinar and ductal cells (Fig. 1C). Moreover, an increased amount of IL-25 expressing cells was observed surrounding the lymphocytic infiltration in the SG of ESS mice. To investigate whether increased IL-25 production results in enhanced IL-17RB expression, we determined the IL-17RB expression on $CD4^+$ T cells obtained from SG lymphoid infiltrates, SG draining cervical lymph nodes (CLN) and spleen (SP). SG-infiltrating $CD4^+$ T cells showed a strong upregulation of IL-17RB, which was observed also significantly upregulated in the ESS CLN compared with naïve mice (Figure 1D). Since the binding of IL-17RB to TNF receptor associated factor 6 (TRAF6) is critical for the signaling transduction of IL-25,[15] we further determined the intracellular expression of TRAF6. In ESS mice, enhanced TRAF6 expression was detected in the $IL\text{-}17RB^+$ subpopulation of $CD4^+$ T cells in the infiltrates,

compared with IL-17RB$^-$ subpopulations (Fig. 1E), indicating an IL-25/IL-17RB/TRAF6 axis in autoreactive T cell activation.

*Histologic evaluation of pSS patients*

On the basis of the histological evaluation, we identified in pSS patients a median biopsy focus score (FS) of 6.44 (range 1–11), while no foci were observed in patients with nSS. Ectopic lymphoid structures comprising CD3$^+$, CD20$^+$ and CD21$^+$ cells were observed in 17 (34%) patients, the remaining showing diffuse lymphocytic infiltrates. All the lymphoma cases included in the study were low-grade marginal zone B cell NHL of the mucose-associated lymphoid tissue (MALT) type, thus with lymphoepithelial lesions. The B phenotype of each lymphoma was confirmed using the pan-B antibody CD20.

*IL-25 axis is activated in pSS patients*

To evaluate how IL-25/IL-17RB axis relates to local pathology, MSG obtained from patients and controls were evaluated for IL-25, IL-17RB and IL-17B expression. Elevated transcripts levels for IL-25 (Figure 2A) were observed in pSS MSG compared to controls and accompanied by the significant up-regulation of IL-17RB (Figure 2B) but not of IL-17B (Figure 2C). In particular, IL-25 expression was significantly correlated with lymphocytic FS ($r^2$=0.36, p<0.0001) and the presence of GCs (data not shown). To validate the RT-PCR data, expression of IL-25, IL17RB and IL-17B was also assessed by immunohistochemistry. Consistent with the mRNA data, augmented expression of IL-25 (Figure 2D-G) and IL-17RB (Figure 2H-K), but not of IL-17B (Figure 2L-O), was observed in pSS patients compared with control tissue. IL-25 expression was mainly observed among infiltrating mononuclear cells, epithelial cells and high endothelial venules in close proximity to areas of lymphocytic infiltration (Figure 2D-E). MSG were also graded histologically and the number of IL-25$^+$ cells was significantly correlated with the FS ($r^2$=0.32, p<0.0001) (data not shown), showing the biopsies with ectopic lymphoid

structures the highest number of IL-25$^+$ cells. Consistent with IL-25 tissue distribution, IL-17RB expression was largely observed in T cell–rich areas of lymphoid aggregates but not in epithelial cells (Fig. 2H-I). In order to characterize IL-17RB$^+$ cells, flow cytometry was performed on isolated peripheral blood mononuclear cells (PBMC) and SGMC. As shown in figure 3A-C, IL-17RB was expressed on the surface of CD3$^+$, CD19$^+$ and CD68$^+$ cells, expecially among SGMC. To demonstrate the functional relevance of IL-25/IL-17RB interaction, we also studied the expression of TRAF6 by immunohistochemistry and confocal microscopy, since that the activation of TRAF6 is critical for the IL-17RB signal transduction (15). TRAF6 was overexpressed in the inflamed SG of patients with pSS (Figure 3E-F) compared to nSS (Figure 3D), mainly expressed among IL-17RB$^+$ cells (Figure 3G-I). These findings suggest that selective activation of IL-17RB, on effector immune cells, by IL-25 is associated with MSG inflammation.

*Higher frequency of IL-25-responsive iILC2 in both SGMC and PBMC of pSS.*

Since the increased expression of IL-25 and IL-17RB, we next evaluated the frequencies of natural (nILC2) and inflammatory ILC2 cells by flow cytometry in both SGMC and PBMC. As shown in Supplemental figure 1 nILC2, defined as lin$^-$CD45$^+$CRTH2$^+$GATA3$^+$IL-4$^+$ cells, were not significantly expanded in pSS patients compared to controls (Supplemental figure 1 A-C). Conversely, a significantly increased frequency of iILC2, defined as lin$^-$(ST2$^-$)CD45$^+$IL-25R$^+$KLRG1$^+$Thy1$^+$ cells, was observed in both SG and peripheral blood (Figure 4 A-C) of pSS. SG iILC2 cells were significantly correlated with the FS (Figure 4D) whereas circulating iILC2 cells were correlated with the disease activity evaluated by ESSDAI (Figure 4E). Interestingly the percentages of iILC2 cells were also significantly correlated with the percentage of IL-25-expressing cells ($r^2$=0.32, p<0.0001) (data not shown). We next evaluated by confocal microscopy the tissue distribution of ILC2 cells by analyzing Thy1, IL-17RB and CD3 expression in pSS patients and controls. Both diffuse distribution (not shown) and the presence of aggregates of Thy1$^+$/IL-17RB$^+$/CD3$^-$ cells

(Figure 4F-I) were observed in the MSG of pSS. Since that ARG-1 activity has been demonstrated to profoundly influence ILC2 ability to proliferate and exert pro-inflammatory functions (16), expression of ARG-1 was assessed in the inflamed SG of pSS and nSS. ARG-1 expression was significantly up-regulated in pSS compared to control subjects (Supplemental figure 1D). Finally, since that activated ILC2 cells have been demonstrated to produce high levels of IL-5 and IL-13 (17), we also evaluated their expression levels in MSG of patients and controls. As shown in Supplemental figure 1E and F, both IL-5 and IL-13 were significantly over-expressed in pSS.

*M2 macrophages are expanded in the salivary glands, but not in the peripheral blood, of pSS patients*

IL-25 and ILC2 have been demonstrated to induce alternatively activated (M2) macrophages (7-8, 18). Thus we next evaluated the frequency of M2 macrophages in both MSG and peripheral blood. As shown in figure 5, a significant expansion of $CD163^+$ macrophages was observed in pSS SG (Figure 5A-D). Since that M2 macrophages are better defined by the co-expression of different markers such as CD163 and cMAF (19), double immunostaining was performed and the sections analyzed by confocal microscopy. As shown in figure 5E-G, $CD163^+cMAF^+$ cells were expanded in pSS MSG. Interestingly, no expansion of M2 macrophages was observed in the peripheral blood of pSS patients compared to controls (data not shown).

*IL-25 induces the expansion of iILC2 and the production of autoantibodies in pSS*

In order to study the effect of IL-25 on ILCs and macrophage polarization, PBMC were isolated and co-coltured in the presence or not of IL-25. IL-25 induced a significant expansion of iILC2 (Figure 5H-I), but not of nILC2 and/or M2 monocytes (data not shown), between isolated PBMC. Since that IL-25 has been found to activate signaling pathways in B cells *in vitro* (20), we also studied the effect of recombinant IL-25 on the production of anti-RoSSa and LaSSb antibodies. As shown in figure 5J, after IL-25 stimulation of PBMC

we documented significant increased levels of anti-RoSSA in surnatants of cultured PBMC from pSS patients.

*IL-25 neutralization attenuated disease progression and tissue pathology in ESS mice*

To investigate whether IL-25 can be targeted for therapeutic purposes in pSS, we performed IL-25 neutralization in established ESS mice. ESS mice at 20wk post immunization (diagnosed with decreased salivary function and lymphocytic infiltration in the SG, histological score = 1) received PBS vehicle or IL-25 monoclonal antibody (200 μg per mouse, twice every week) for 4 weeks and examined at 30wk post immunization, while the histological changes of SG were assessed. Although severe tissue destructions with multiple foci developed in the SG of vehicle-treated ESS mice, IL-25 neutralization profoundly inhibited the exacerbation of disease pathology (Fig. 6A). Notably, blockade of IL-25 resulted in reduced lymphocytic infiltration and foci numbers upon the ESS progression. The saliva flow rate of ESS mice after anti-IL-25 treatment was only mildly and not significantly improved (p=0.06) (data not shown). A significant reduction of IL-5, but not IL-13, was also observed in ESS mice with anti-IL-25 treatment (Supplemental Figure 1 G-H). It was reported that IL-25 suppressed IFN-γ production during colitis (21). Consistently, SG-infiltrating Th1 cells were markedly decreased upon IL-25 neutralization (Fig. 6B). Similar to the findings in human pSS, we also detected increased $CD45^{+}Lin^{-}IL\text{-}17RB^{+}IL\text{-}7R\alpha^{+}$ ILC2 in the SG of diseased ESS mice. However, ESS mice treated with anti-IL-25 showed significantly reduced frequencies and cell numbers of ILC2 (Fig. 6C). In addition, IL-25 neutralization was shown to selectively inhibit the $CD206^{+}F4/80^{+}$ M2 macrophages among the lymphocytic infiltration (Fig. 6D). Thus, our findings suggested that IL-25 might serve as a therapeutic target for the treatment of pSS.

*Rituximab modulates salivary gland IL-25 expression and iILC2 in pSS patients*

Rituximab has been demonstrated to modulate local and systemic immune responses in pSS patients and the function of innate immune cells such as NK cells (22-23). We finally evaluated the local expression of IL-25 and the peripheral frequencies of iILC2 and M2 macrophages in 5 pSS patients after Rituximab therapy. As shown in Suppl figure 2, Rituximab treatment was associated with a significant reduction of SG IL-25 expression levels (Suppl Figure 2A-B) and of percentage of circulating iILC2 cells (Suppl Figure 2 C-D) but not of M2 macrophages (data not shown).

*IL-25/IL-17RB axis is activated in pSS-associated lymphoma*

Since that IL-25 regulates hematopoietic and immune functions (24), stimulating the development of B lymphocytes, we next evaluated the involvement of IL-25/IL-17RB axis in pSS-associated SG MALT lymphoma tissues. As shown in Supplemental Figure 2, a significant over-expression of IL-25 was observed in SG samples with lymphoma (Suppl Figure 2E) and was accompanied by a significant over-expression of IL-17RB (Suppl Figure 2F) and of TRAF6 (Suppl Figure 2G), indicating the activation of IL-25/IL-17RB axis also in pSS-associated lymphomas.

**Discussion**

In this study, we provide for the first time evidences that IL-25/IL-17RB axis is activated in pSS patients and in mice with SS and associated with the selective expansion of specific subsets of ILC2 and the occurrence of a M2 polarization. We also demonstrate that the neutralization of IL-25 causes a decrease in the progression of disease in a murine model of SS thus representing a possible successful strategy in the treatment of SS.

IL-25 is an important molecule controlling innate and adaptative immunity (4). IL-25 signals through the IL-17RB receptor that specifically binds to IL17B and IL25, but does not bind to IL17A or IL17C (4). Interaction of IL-17B and IL-25 with IL-17RB induces different biologic activities. IL-17B, in fact, essentially acts on epithelial cells inducing the expression of IL-8 and the up-regulation of pro-inflammatory chemokines such as CXCL1, CCL20 and TFF1 via the ERK1/2 pathway (25). Conversely, IL-25/IL-17RB interaction essentially regulates B cell function, induces autoimmune Th17-driven inflammation and promotes Th2 responses, by increasing the frequency of M2-polarized macrophages and the differentiation of type 2 innate lymphoid cells cell (ILC2) (6-7,9,20).

In pSS, IL-17RB was almost exclusively observed on the surface of inflammatory immune cells infiltrating pSS SG with very low expression in ductal and/or acinar epithelial cells, indicating a predominant role of this receptor in modulating the function of infiltrating inflammatory cells. According to the expression of IL-17RB on immune cells, we demonstrated that IL-25, but not IL-17B, is over-expressed in pSS SG with a distribution that followed that of IL-17RB. Over-expression of human IL-25 has been demonstrated to result in lymph node medullary expansion due to increase of reactive B cells, plasma cells

and macrophages (26). In line with these results, in our study, IL-25 expression was correlated with the lymphocytic FS and with the degree of GCs organization. IL-17RB is known to interact with TNF receptor associated factor 6 (TRAF6) and ACT1, and TRAF6-TAK1 activates the ERK–MAPK signaling for cell survival (15). In pSS SG, we observed a significant up-regulation of TRAF6, especially among $CD3^+$ and ILC2 cells indicating that IL-25/IL-17RB signaling is functional in pSS via coordinated activation of ERK1/2 and its downstream transcription factors. In the seminal study published by Huang Y et al (8) it has been demonstrated that IL-25-dependent iILC2s also express high levels of GATA-3, more than nILC2, and an intermediate amount of RORγt, less than ILC3 cells, but significantly distinct from nILC2s. The exact contribution of these different transcription factors in modulating ILC2 expansion needs to be better clarified in future studies. IL-25/IL-17RB/TRAF6 axis was also studied in SG protein-immunised ESS mice, a murine model of SS. In ESS, serum levels of IL-25 were significantly increased at 30wk post-immunization and, similarly to human pSS, we detected increased numbers of IL-25 producing cells in the SG of ESS mice with glandular infiltration. Interestingly, $IL\text{-}25^+$ tissue cells were mainly found surrounding glandular-infiltrating $CD4^+$ T cells. Increased IL-17RB expression was also demonstrated in glandular-infiltrating $CD4^+$ T cells, as well as enhanced TRAF6 expression in $IL\text{-}17RB^+CD4^+$ T cell sub-populations. Altogether these findings seem to indicate a critical role of IL-25 axis in the pathogenesis of pSS and ESS.

IL-25/IL-17RB expression has been proved to induce the expansion of M2 macrophages, and type 2 innate lymphoid cells (7-8). ILC2s require ROR-A and GATA3 for their development and together with IL-25, IL-33 has been also demonstrated to be the predominant ILC2-inducing cytokine (17). Recently, it has been reported the existence of an inflammatory ILC2 population responsive to IL-25 that complemented IL-33-responsive natural ILC2 cells (8). iILC2 cells developed into nILC2-like cells *in vitro* and *in vivo* and acquire IL-17-producing ability (27). In this regard, IL-33 has been recently demonstrated

to be over-expressed in pSS patients (3). In our study, a strong and significant expansion of iILC2 was observed in pSS at both peripheral and local levels, significantly correlated with the FS, the disease activity evaluated by ESSDAI and the number of infiltrating IL-25$^+$ cells. Conversely, nILC2 cells were not significantly expanded neither in the MSG and peripheral blood of pSS. The role of IL-25 in modulating the iILC2 expansion in pSS seems to be confirmed by the demonstration that IL-25 addition to isolated SGMC and PBMC was able *in vitro* to selectively induce the expansion of iILC2. Interestingly, iILC2 cells may be transient progenitors of ILCs mobilized by inflammation and infection that develop into nILC2-like cells or ILC3-like cells contributing to immunity to helminths and fungi (27). Since that ILC3s producing IL-22 have been demonstrated to be expanded in pSS patients (12), contributing to the pathogenesis of pSS, we can not obviously exclude that a proportion of SG iILC2 may become ILC3.

IL-25-activated-ILC2 have been demonstrated to produce Th2 cytokines such as IL-5 and IL-13 (17). According to the presence of ILC2 in the SGof pSS patients, high levels of the Th2 cytokines, IL-5 and IL-13, were observed. Th2 cytokines have been demonstrated to elicit specific M2 macrophage responses (28). Macrophages play essential activities in homeostasis maintenance, being differently polarized according to various stimuli into 2 distinct populations of M1 and M2 macrophages (28). According to the IL-25 over-expression and iILC2 polarization, we observed a clear expansion of M2 macrophages in both SGand peripheral blood of pSS. In pSS SG, M2 macrophages were demonstrated as CD163$^+$cMAF$^+$ cells, since that the only presence of CD163 is not sufficient to define M2 polarization, and their number was correlated with the FS.

IL-25 regulates hematopoietic and immune functions specifically stimulating B lymphocytes expansion in spleen, lymph nodes, and other secondary lymphohematopoietic tissues (20). Our demonstrations that IL-25 is able to induce *in vitro* the production of pSS associated autoantibodies and that IL-25 axis is upregulated also in

pSS-associated MALT lymphomas patients seem to support the importance of IL-25 in modulating B cell function. The B cells response observed in our in vitro studies after IL-25 stimulation might be modulated by TRAF6 over-expression since that it has been demonstrated that TRAF6 is required for both T-dependent and T-independent B cell response (29). Other pathways however might be involved in the autoantibody production and their exact contributions need further functional studies. Finally, our demonstration that depletion of B cells by Rituximab in pSS patients significantly reduces the local levels of IL-25 and the frequency of circulating iILC2 may indirectly suggest that modulation of IL-25 axis might be also relevant in the treatment of these patients. In this regard, Rituximab has been demonstrated to modulate innate and adaptive immune responses in pSS patients beyond the B-cell depletion. In particular depletion of $CD20^+$ T cells (30), mast cells (31) and reduction in the expression of different cytokines such as IL-22 (32) and IL-17 (31) has been demonstrated after RTX therapy. Consistent to this hypothesis is our demonstration that neutralization of IL-25 resulted in reduced lymphocytic infiltration and foci numbers upon the ESS progression and in the significant reduction of infiltrating Th1 cells, of CD45+Lin-IL-17RB+IL-7Rα+ ILC2 and of CD206+F4/80+ M2 macrophages.

In conclusion, in this study we provide the first demonstration that IL-25/IL-17RB axis is activated in pSS patients, in pSS-associated MALT lymphomas and in ESS. In pSS patients the activation of this axis is associated with the expansion of iILC2 and M2 macrophages. Targeting of this axis might be relevant in treating pSS patients.

**Acknowledgements**: we would like to deeply thank Dr Francesca Raiata (Sezione di Anatomia Patologica, Azienda Ospedaliera Ospedali riuniti Villa Sofia Cervello, Palermo, Italy) for her technical support in immunohistochemical experiments.

**Funding sources**: this study was in part supported by a grant of Ministero dell'Istruzione, dell'Università e della ricerca Scientifica from Italy. This work was also supported by grants

from National Natural Science Foundation of China (31300739), Hong Kong Research Grant Council General Research Fund (17149716) and Croucher foundation (260960116).

**Figure Legends**

**Figure 1. Enhanced IL-25 responses during experimental Sjögren's syndrome (ESS) development.** (A) Kinetic changes of IL-25 in the sera of ESS were measured by ELISA assay (n=6 per time point); (B) IL-25-producing cells were detected among the SG $CD45^-$ tissue cells by flow cytometry. Obvious elevation of IL-25-producing cells were found in the SG of ESS mice with severe lymphocytic infiltration, while no significant change was detected in those ESS mice without infiltration and normal controls; IL-25-producing tissue cells were enumerated in the SG of control and in ESS mice (n = 4 for each group); (C) Intracellular staining of IL-25 cells in the SG of control mice was detected by confocal microscopy (on the left). In ESS mice (on the right), an increased number of IL-25-expressing cells was observed compared to control mice, mostly localized in the area immediately surrounding the lymphocytic foci, bar = 20 μm; (D) Phenotypic analysis of IL-17RB expression on $CD4^+$ T cells by flow cytometry. The frequency of IL-$17RB^+CD4^+$ T cells was summarized for comparison; (E) Mean fluorescence intensity of TRAF6 staining within IL-$17RB^+$ and IL-$17RB^-$ populations of SG-infiltrating $CD4^+$ T cells. Data are derived from three separate experiments (mean±SD; ns, no significance $P>0.5$; *$P<0.05$, **$P<0.01$ and ***$P<0.001$).

**Figure 2: IL-25, IL-17RB and IL-17B in salivary glands of pSS patients.** A-C: Relative m-RNA quantification of IL-25 (A), IL-17RB(B) and IL-17B (C) was assessed by quantitative RT-PCR in SG samples obtained from 50 pSS patients and 20 control subjects. A significant over-expression of IL-25 (A) and IL-17RB(B) but not of IL-17B (C) was observed only in pSS patients. D-F: Representative microphotographs showing IL-25 immunostainings in pSS subjects (D-E) and controls (F). G: IL-25 semiquantitative score in

the SG of pSS patients and controls. H-J: Representative microphotographs showing IL-17RB immunostainings in pSS subjects (H-I) and controls (J). K: IL-17RB semiquantitative score in the SG of pSS patients and controls. L-N: Representative microphotographs showing IL-17B immunostainings in pSS subjects (L-M) and controls (N). O: IL-17B semiquantitative score in the SG of pSS patients and controls. Significant over-expression of IL-25 and IL-17RB, but not of IL-17B was detected only in pSS patients. D-F, H-J, L-N: original magnification x 250. Data are expressed as individual data points.

**Figure 3: IL-17RB is over-expressed among PBMC and SGMC of pSS patients and accompanied by TRAF-6 increased expression.** A: Representative dot plots showing gating strategy and IL-17RB expressing cells among PBMC and SGMC of pSS patients. Percentages of IL-17RB-expressing cells among PBMC (B) and SGMC (C) in pSS and nSS. Data are expressed as individual mean (SEM). D-F: representative images showing TRAF6 immunostaining in nSS (D) and pSS patients (E-F). G-I: confocal microscopy analysis of IL-17RB and TRAF6 in pSS SG showing the perfect co-localization of IL-17RB and TRAF6. G: single staining for IL-17RB; H: single staining for TRAF6; I: merge double staining for 17RB and TRAF6. C-H: original magnification x 250

**Figure 4: Inflammatory ILC2 (iILC2) in pSS patients.** Salivary glands (SGMC) and peripheral blood mononuclear cells (PBMC) were analyzed by flow cytometry in pSS patients and controls. A: Representative dot plots showing gating strategy and the percentages of iILC2 in SGMC and PBMC of pSS patients. B: percentages of iILC2 among SGMC in pSS and nSS. C: percentages of iILC2 in pSS and nSS. The percentages of iILC2 were significantly expanded in the salivary glands and in the peripheral blood of pSS patients. D: correlation between the percentages of SG iILC2 and the focus score. E: correlation between the percentages of circulating iILC2 and the disease activity evaluated by ESSDAI. Data are expressed as individual data points. F-I: confocal microscopy analysis of iILC2 in pSS SG showing the presence of aggregate of ILC2. F: single staining

for Thy1; G: single staining for IL-17RB; H: single staining for CD3; I: merge triple staining for Thy1, IL-17RB and CD3. F-I: original magnification x 250.

**Figure 5: M2 macrophages in salivary glands of pSS and role of IL-25 in *in vitro* expansion of iILC2 and on the levels of anti-RoSSA antibodies in pSS patients.** A-C: Representative microphotographs showing CD163 immunostainings in pSS subjects (A-B) and controls (C). D: semiquantitative evaluation of $CD163^+$ cells in pSS and in nSS. E: single staining for CD163; F: single staining for cMAF; G: merge double stainig for CD163 and cMAF. A-C and E-G: original magnification x250. Data are expressed as individual data points. H: representative dot-plots showing the frequency of iILC2 with or without incubation with recombinant IL-25. I: percentage of iILC2 after incubation of PBMC with recombinant IL-25. The results are shown as the mean of 5 different expetiments. J: titre of anti-RoSSa antibodies before and after treatment of isolated PBMC with rIL-25; results are shown as the mean of 5 different experiments. Data are expressed as mean (SEM).

**Figure 6. IL-25 neutralization attenuated disease progression and tissue pathology in ESS mice.** (A) Histological assessment of SG by H&E staining, n = 7 per group, bar = 100 μm; Lymphocytic foci were assessed for histological scores; (B) Gated on $CD45^+CD4^+$ T cells, representative flow cytometric analysis of Th1 cells in the SG of ESS mice and the cell numbers were summarized; (C) Gated on $CD45^+Lin^-$ population, representative flow cytometric analysis of $IL\text{-}17RB^+IL\text{-}7R\alpha^+$ ILC2 in the SG of ESS mice was shown and the cell numbers were summarized; (D) Gated on $CD45^+F4/80^+$ population, representative flow cytometric analysis of $CD11c^+CD206^-$ M1 macrophages and $CD11c^-CD206^+$ M2 macrophages in the SG of ESS mice was shown and the cell numbers were summarized. (Mean±SD; *P<0.05 and **P<0.01).

**Supplemental Figure 1:** A: Representative dot plots showing gating strategy and the percentages of nILC2 in SGMC and PBMC of pSS patients. B: percentages of nILC2 among SGMC in pSS and nSS. C: percentages of nILC2 among PBMC in pSS and nSS.

D-F: Relative m-RNA quantification of ARG-1 (D), IL-5 (E) and IL-13 (F) was assessed by quantitative RT-PCR in SG samples obtained from 50 pSS patients and 20 control subjects. Data are expressed as individual data points.

**Supplemental Figure 2:** A: representative images showing reduction of IL-25 expression in the MSG of pSS after Rituximab therapy. B: semiquantitative evaluation of the number of IL-25$^{+}$ cells before and after Rituximab therapy. C: representative dot-plots showing the frequency of iILC2 in a patient with pSS after RTX therapy. D: percentages of iILC2 among PBMC in 5 pSS patients treated with Rituximab. E-G: IL-25 axis in pSS associated lymphoma. E-G: representative images showing IL-25 (E), IL-17RB (F) and TRAF6 (G) immunostaining in a patient with pSS-associated MALT lymphoma. A, E-G: original magnification x 250. Data are expressed as mean (SEM)

**References**


1. Mavragani CP and Moutsopoulos HM. Sjogren's syndrome. Ann Rev Pathol 2014;9: 273-285
2. Maehara T, Moriyama M, Hayashida JN, Tanaka A, Shinozaki S, Kubo Y et al. Selective localization of T helper subsets in labial salivary glands from primary Sjogren's syndrome patients. Clin Exp Immunol 2012;169:89–99.
3. Awada A, Nicaise C, Ena S, Schandéné L, Rasschaert J, Popescu I et al. Potential involvement of the IL-33-ST2 axis in the pathogenesis of primary Sjogren's syndrome. Ann Rheum Dis 2014;73:1259-63.
4. Iwakura Y, Ishigame H, Saijo S, Nakae S. Functional specialization of interleukin-17 family members. Immunity 2011;34:149-62.
5. Gaffen S. IL-17 receptor composition. Nat Rev Immunol 2016;16(1):4.
6. Kleinschek MA, Owyang AM, Joyce-Shaikh B, Langrish CL, Chen Y, Gorman DM et al. IL-25 regulates Th17 function in autoimmune inflammation. J Exp Med 2007;204:161-70.
7. Cao Q, Wang C, Zheng D, Ya Wang, Vincent W. S. Lee, Yuan Min Wang et al. IL-25 induces M2 macrophages and reduces renal injury in proteinuric kidney disease. J Am Soc Nephrol 2011;22:1229-39.
8. Huang Q, Niu Z, Tan J, Jun Yang, Yun Liu, Haijun Ma et al. IL-25 Elicits Innate Lymphoid Cells and Multipotent Progenitor Type 2 Cells That Reduce Renal Ischemic/Reperfusion Injury. J Am Soc Nephrol 2015;26:2199-211.
9. Huang Y, Guo L, Qiu J, Chen X, Hu-Li J, Siebenlist U et al. IL-25-responsive, lineage-negative KLRG1(hi) cells are multipotential 'inflammatory' type 2 innate lymphoid cells. Nat Immunol 2015;16:161-9.

10. Lin X, Rui K, Deng J, Tian J, Wang X, Wang S et al. Th17 cells play a critical role in the development of experimental Sjögren's syndrome. Ann Rheum Dis 2015;74:1302-10.
11. Vitali C, Bombardieri S, Jonsson R, Moutsopoulos HM, Alexander EL, Carsons SE et al. Classification criteria for Sjogren's syndrome: a revised version of the European criteria proposed by the American-European Consensus Group. Ann Rheum Dis 2002; 61:554-558.
12. Greenspan, J, Daniels, T, Talal, N and Sylvester, RA. The histopathology of Sjögren's syndrome in labial biopsies. Age Ageing 1974; 1:197.
13. Ciccia F, Guggino G, Rizzo A, Bombardieri M, Raimondo S, Carubbi F et al. Interleukin (IL)-22 receptor 1 is over-expressed in primary Sjogren's syndrome and Sjögren-associated non-Hodgkin lymphomas and is regulated by IL-18. Clin Exp Immunol 2015;181:219-29
14. Mach PS, Kharouby M, Lutcher F, Olivier JL, Bazely N, Dougados M et al. The in vitro production of anti-nuclear antibodies by human peripheral blood mononuclear cells. Demonstration of T cell requirement and soluble inducing factor(s) for anti-nuclear antibodies triggering in patients with systemic lupus erythematosus. Clin Exp Immunol 1984; 54:535-40
15. Maezawa Y, Nakajima H, Suzuki K, Tamachi T, Ikeda K, Inoue J et al. Involvement of TNF receptor-associated factor 6 in IL-25 receptor signaling. J Immunol 2006;176:1013-8.
16. Monticelli LA, Buck MD, Flamar AL, Saenz SA, Tait Wojno ED, Yudanin NA et al. Arginase 1 is an innate lymphoid-cell-intrinsic metabolic checkpoint controlling type 2 inflammation. Nat Immunol 2016;17:656-65.
17. Klose CS, Artis D. Innate lymphoid cells as regulators of immunity, inflammation and tissue homeostasis. Nat Immunol 2016;17:765-74

18. Bouchery T, Kyle R, Camberis M, Shepherd A, Filbey K, Smith A et al. ILC2s and T cells cooperate to ensure maintenance of M2 macrophages for lung immunity against hookworms. Nat Commun 2015;6:6970
19. Barros MHM, Hauck F, Dreyer JH Kempkes B, Niedobitek G et al. Macrophage Polarisation: an Immunohistochemical Approach for Identifying M1 and M2 Macrophages. PLoS ONE 2013; 8: e80908.
20. Benatar T, Cao MY, Lee Y, Lightfoot J, Feng N, Gu X et al. IL-17E, a proinflammatory cytokine, has antitumor efficacy against several tumor types in vivo. Cancer Immunol Immunother 2010;59:805-17
21. Caruso R, Sarra M, Stolfi C, Rizzo A, Fina D, Fantini MC, et al. Interleukin-25 inhibits interleukin-12 production and Th1 cell-driven inflammation in the gut. Gastroenterology. 2009 Jun; 136:2270-2279.
22. Ciccia F, Guggino G, Rizzo A, Alessandro R, Carubbi F, Giardina A et al. Rituximab modulates IL-17 expression in the salivary glands of patients with primary Sjögren's syndrome. Rheumatology (Oxford) 2014;53:1313-20
23. Ciccia F, Giardina A, Rizzo A, Guggino G, Cipriani P, Carubbi F et al. Rituximab modulates the expression of IL-22 in the salivary glands of patients with primary Sjogren's syndrome. Ann Rheum Dis 2013;72:782-3.
24. Wang YH, Angkasekwinai P, Lu N Voo KS, Arima K, Hanabuchi S et al. IL-25 augments type 2 immune responses by enhancing the expansion and functions of TSLP-DC-activated Th2 memory cells. J Exp Med 2007;204:1837-47.
25. Wu HH, Hwang-Verslues WW, Lee WH, Huang CK, Wei PC, Chen CL et al. Targeting IL-17B-IL-17RB signaling with an anti-IL-17RB antibody blocks pancreatic cancer metastasis by silencing multiple chemokines. J Exp Med. 2015;212:333-49.

26. Kim MR, Manoukian R, Yeh R, Scott M. Silbiger, Dimitry M. Transgenic overexpression of human IL-17E results in eosinophilia, B-lymphocyte hyperplasia, and altered antibody production. Blood 2002;100:2330-2340

27. Lim AI, Menegatti S, Bustamante J, Le Bourhis L, Allez M, Roggeet L et al. IL-12 drives functional plasticity of human group 2 innate lymphoid cells. J Exp Med 2016;213:569-83.

28. Wang N, Liang H, Zen K. Molecular mechanisms that influence the macrophage m1-m2 polarization balance. Front Immunol. 2014 Nov 28;5:614.

29. Kobayashi T, Kim TS, Jacob A, Walsh MC, Kadono Y, Fuentes-Pananá E et al. TRAF6 is required for generation of the B-1a B cell compartment as well as T cell-dependent and -independent humoral immune responses. PLoS One. 2009;4(3):e4736. doi: 10.1371/journal.pone.0004736.

30. Mélet J, Mulleman D, Goupille P, Ribourtout B, Watier H, Thibault G. Rituximab-induced T cell depletion in patients with rheumatoid arthritis: association with clinical response. Arthritis Rheum 2013;65:2783-90.

31. Ciccia F, Guggino G, Rizzo A, Alessandro R, Carubbi F, Giardina A et al. Rituximab modulates IL-17 expression in the salivary glands of patients with primary Sjögren's syndrome. Rheumatology (Oxford) 2014;53:1313-20.

32. Ciccia F, Giardina A, Rizzo A, Guggino G, Cipriani P, Carubbi F et al. Rituximab modulates the expression of IL-22 in the salivary glands of patients with primary Sjogren's syndrome. Ann Rheum Dis. 2013 May;72(5):782-3.

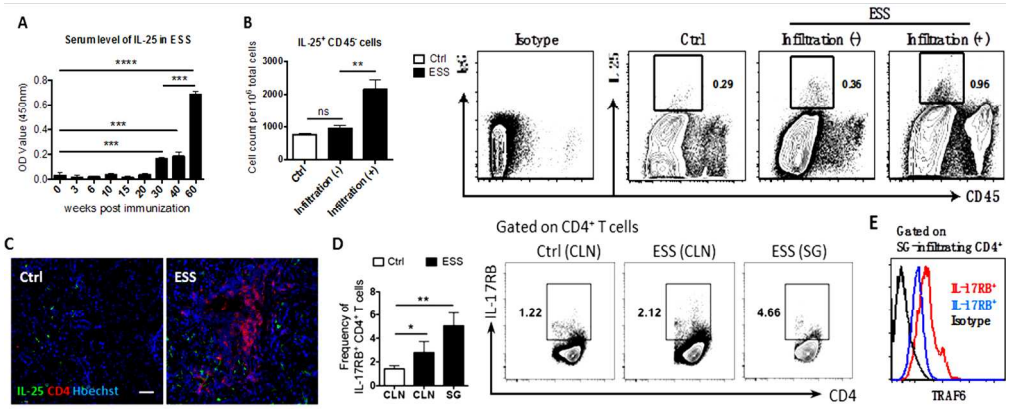


177x72mm (300 x 300 DPI)

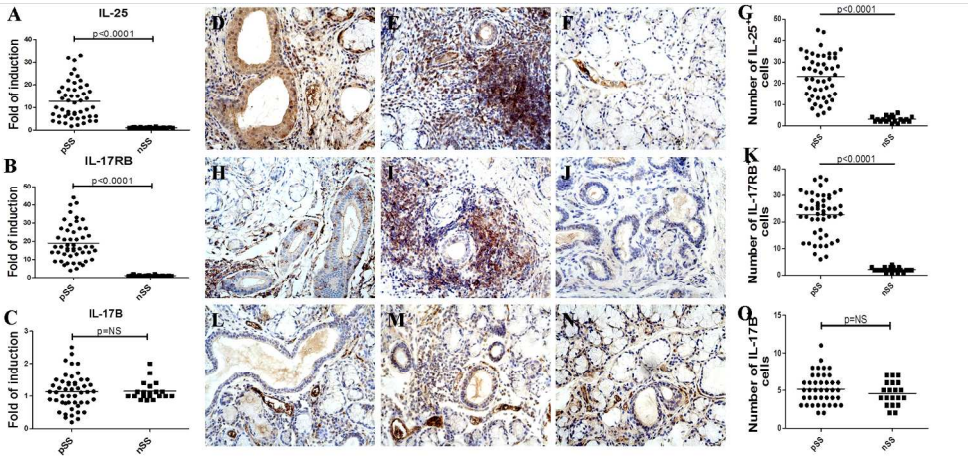


176x81mm (300 x 300 DPI)

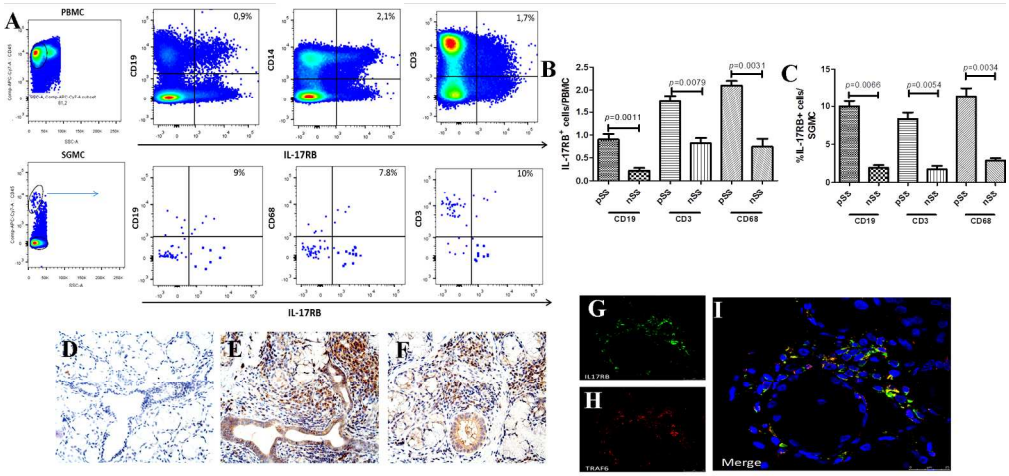


176x83mm (300 x 300 DPI)

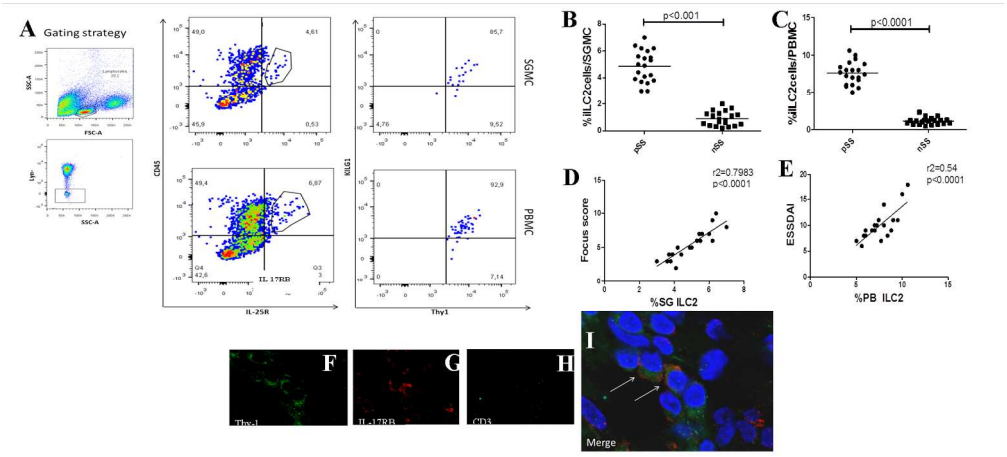


176x81mm (300 x 300 DPI)

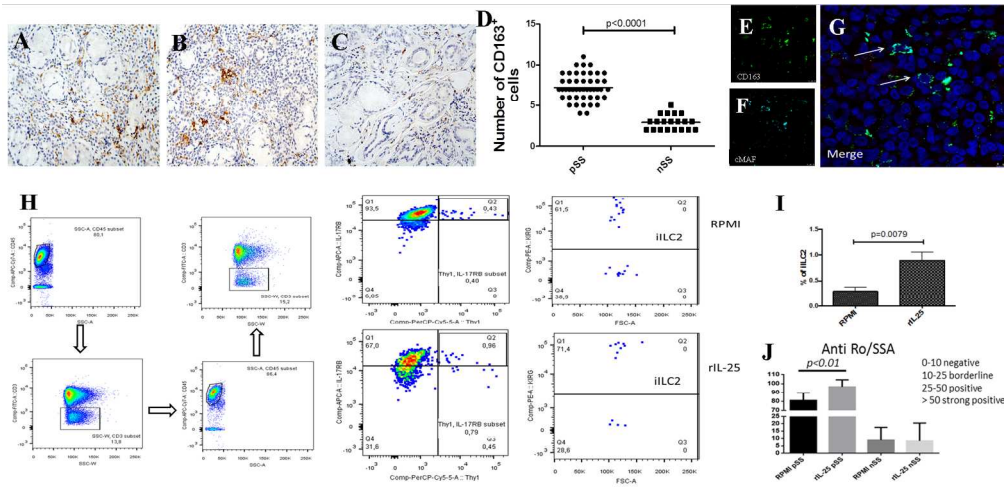


176x85mm (300 x 300 DPI)

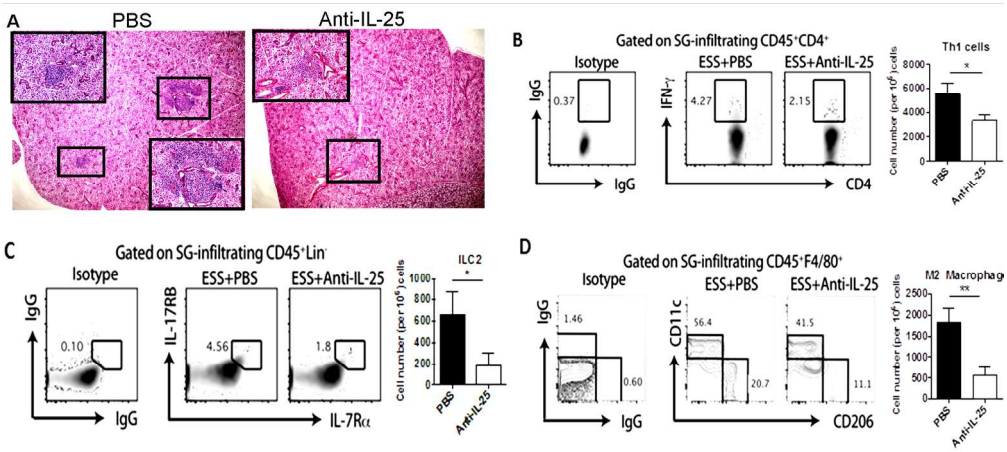


177x79mm (300 x 300 DPI)

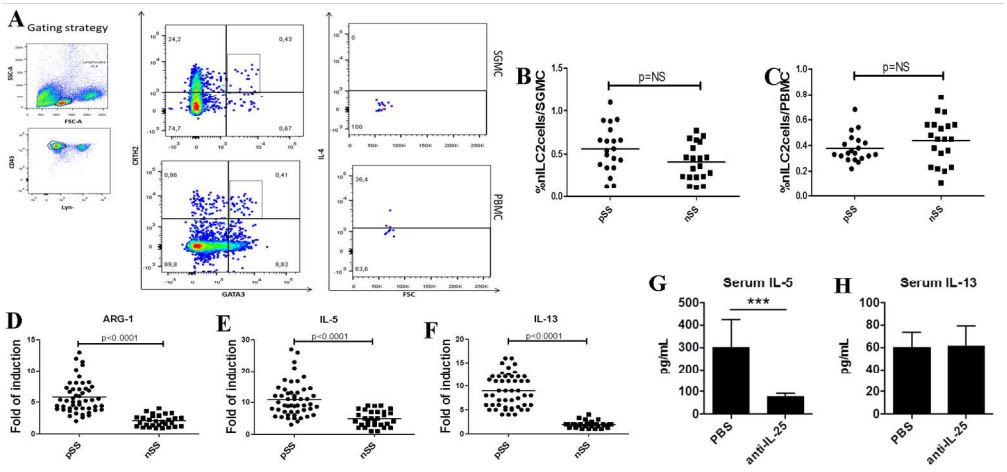


175x81mm (300 x 300 DPI)

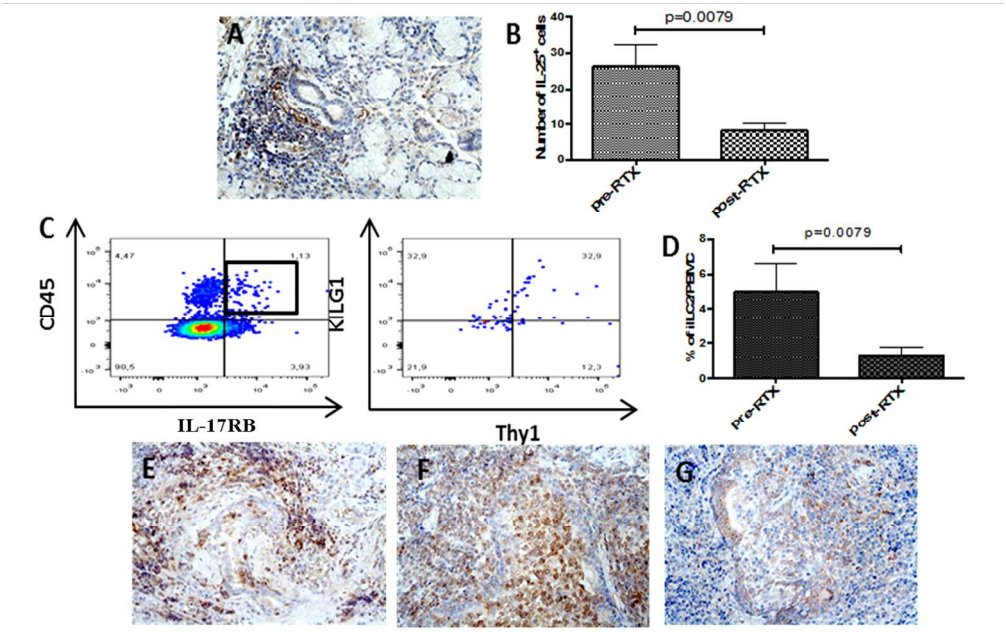


135x85mm (300 x 300 DPI)

Supplemental Table 1: Baseline characteristic of patients and controls

| | pSS N=50 | nSS N=30 | *P* |
|---|---|---|---|
| Age (years), Median (Range) | 58 (21-66) | 54 (25-60) | 0.32 |
| Female sex, n (%) | 48 (96) | 25 (83) | 0.11 |
| Disease duration (months) range | 14 (8-18) | - | - |
| ANA, % of patients | 76 | 0 | - |
| Anti-Ro and/or anti-LA antibodies, % of patients | 52 | 0 | - |
| HCV, % patients | 0 | 0 | - |
| RF, % of patients | 46 | 0 | - |
| ESR mm/h, mean (S.D.) | 40 (16) | 18 (6) | <0.05 |
| CRP, mg/l, mean (S.D.) | 18 (9) | 3 (2) | <0.05 |

**Supplemental Methods**

*Experimental procedures in ESS*

In brief, proteins extracted from the bilateral SG of normal mice were emulsified in an equal volume of Freund's complete adjuvant (Sigma-Aldrich) to a concentration of 2 mg/ml. For SS induction, each mouse received subcutaneous multi-injections on the back of 0.1 ml of the emulsion on days 0 and 7, respectively. On day 14, the booster injection was carried out with a dose of 1 mg/ml SG proteins emulsified in Freund's incomplete adjuvant (Sigma-Aldrich). All experiments for animal studies were approved by the Committee on the Use of Live Animals in Teaching and Research of the University of Hong Kong).

Serum samples from ESS mice at various disease time points were collected and measured by IL-25 ELISA kit (eBioscience) following the manufactural instruction. ESS mice were administrated with 200 μg of anti-IL-25 monoclonal antibody (35B, Biologend) or PBS vehicle via intraperitoneal injection at 20 wk post first immunization. Mice were treated twice every week for 4 wk. SG tissues removed from immunised mice were frozen into OCT compound (Sakura) and sections were cut at 5 μm thickness. For immunofluorescent microscopy, frozen sections were stained with monoclonal antibodies against mouse CD4 (clone RM4-5, Biolegend) and IL-25 (clone 207702, R&D), while nuclei were counterstained with Hoechst 33258 (CalBioChem). Rat IgG antibody was used for control staining. For the flow cytometry experiments in ESS mice surface markers were identified with following anti-mouse monoclonal antibodies: anti-CD4, anti-IL-17RB (clone 752101, R&D), anti-CD45 (30-F11, Biolegend), anti-F4/80 (BM8), anti-IL-7Rα (A7P34, Biolegend), anti-CD206 (C068C2, Biolegend) and anti-lineage markers (CD2, CD3, CD4, CD8, CD19, B220, Gr-1, CD11b, CD11c, FcεRI and TER119, Biolegend). Detection of intracellular IL-25 and TRAF6 (clone EP591Y, Abcam) was prepared by using a fixation/permeablization buffer set (BD Biosciences). Stained cells were analyzed with a

LSRFortessa flow cytometer (BD Biosciences) while Zombie Aqua™ Live/Dead Cell Discrimination kit (Biolegend) was used to exclude the dead cells. Data were analyzed by FlowJo software (Treest).

*Patients*

Thirthy patients with subjective complains of dry mouth or dry eyes who did not fulfill the AECG criteria and show various degree of mononuclear cell infiltration in the absence of focal organisation were classified as having non-specific chronic sialoadenitis (nSS) and were considered as control group. Paraffin-embedded samples obtained from patients with a previous diagnosis of pSS-associated MALT lymphoma (n=5) were obtained from the biopsy bank of the Pathology Unit of the Ospedale Cervello (Palermo, Italy). Diagnosis of lymphoma was made by the demonstration of sheets or halos of monocytoid B cells and by the demonstration of immunoglobulin(Ig)H and/or IgL chain restriction. Baseline characteristics of patients and controls are shown in Supplemental Table1. All the patients and controls gave their informed consent and the study was approved by the ethical committee of the University of Palermo. Multiple labial MSG biopsies were obtained from all the pSS patients and controls and placed into formalin fixative and RNAlater for immunohistochemistry and reverse transcription–polymerase chain reaction (RT–PCR) analyses, respectively. Twenty paired biopsies, from patients and controls, were also placed in RPMI for isolation of SGMC and used for flow cytometry analysis.

*Histology and immunohistochemistry*

A focus was defined as an aggregate of ≥50 lymphocytes. The focus score was reported as the number of foci per 4 $mm^2$ of tissue, up to a maximum of 12 foci. All patients with pSS presented a biopsy focus score ≥1, whereas the control group had a focus score <1. The presence of GC-like lymphoid structures was determined by the presence of T and B lymphocytes and $CD21^+$ follicular dendritic cells networks on sequentially stained sections. Immunohistochemistry was performed on 5-μm-thick paraffin-embedded sections from SG

as described previously.[13] The primary antibodies mouse anti-human IL-25, rabbit anti-human IL-17RB, rabbit anti-human IL-17B (Novus Biologicals, Littleton, CA) and rabbit anti-human TRAF6 (Abcam, Cambridge, UK) were added and incubated for 1 h at room temperature. Isotype-matched irrelevant antibodies were used as a negative control (AbCam, Cambridge, UK). The number of positive cells was determined by counting the reactive cells on microphotographs obtained from three randomly selected high-power microscopic fields (original magnification ×400).

*RNA extraction from salivary gland biopsies and quantitative TaqMan RT–PCR*

Master mix and Taqman® gene expression assays for glyceraldehyde 3-phosphate dehydrogenase (GAPDH control) and target genes IL-25 (Hs03044841_m1), IL-17RB (Hs00218889_m1), IL-17B (Hs00975262_m1), IL-33 (Hs00369211_m1), Arg-1 (Hs00968979_m1) and GADPH (Hs02758991_g1) were obtained from Applied Biosystems (Foster City, CA, USA). Data were quantified using sds 2.1 software and normalized using GAPDH as endogenous control. Relative changes in gene expression between nSS and pSS samples were determined using the ΔΔCt method. Levels of the target transcript were normalized to a GAPDH endogenous control, constantly expressed in both groups (ΔCt). For ΔΔCt values, additional subtractions were performed between pSS (n = 50) and nSS (n = 20) ΔCt values. Final values were expressed as fold of induction.

*Isolation and culture of minor salivary gland mononuclear cells and flow cytometry*

*In vitro* cultured cells were stained with the following antibodies: anti-human CD45, anti-human Lineage Cocktail (anti-human CD3, anti-human CD56, anti-human CD14, anti-human CD19, anti-human TCR-$\gamma\delta$, anti-human iNKT) anti-human IL-17RB, anti-human KLRG1 and anti-human Thy1, anti human GATA3, anti-human CRTH2, anti-human CD14 and anti-human CD68 (BD, Biolegend and R&D). Detection of intracellular IL-25 (R&D) and TRAF6 (Abcam) was performed using a fixation/permeablization buffer set (BD

Biosciences). Flow cytometry analysis was performed using a fluorescence activated cell sorter (FACS)Canto (BD Biosciences, San Jose, CA, USA). At least 50 000 cells (events), gated on the lymphocyte region, were acquired for each sample and data are presented as a percentage of total alive cells in the CD45 channel.

*Evaluation of anti-RoSSA and LaSSB autoantibodies following IL-25 stimulation*

PBMC were obtained from the peripheral blood of pSS patients after centrifugation on Ficoll-Hypaque (Pharmacia). The medium used throughout was RPMI 1640 (Invitrogen Life Technologies) supplemented with 10% heat-inactivated pooled human AB+ serum, 2 mM l-glutamine, 20 mM HEPES, 100 U/ml penicillin, 100 µg/ml streptomycin, $5 \times 10^{-5}$ M 2-ME. PBMC were cultured with or without recombinant-IL-25 (rIL-25: 0.25 ug/ml) in U-bottom 96-well plates and incubated at 37°C, 5% $CO_2$ for 72 hours. After incubation, supernatants were collected to test anti-RoSSA/LaSSB production by Immunoblot (Euroimmune).